LINEAR MATRIX INEQUALITY APPROACH FOR SYNCHRONIZATION OF CHAOTIC FUZZY CELLULAR NEURAL NETWORKS WITH DISCRETE AND UNBOUNDED DISTRIBUTED DELAYS BASED ON SAMPLED-DATA CONTROL

P. BALASUBRAMANIAM, K. RATNAVELU AND M. KALPANA

ABSTRACT. In this paper, linear matrix inequality (LMI) approach for synchronization of chaotic fuzzy cellular neural networks (FCNNs) with discrete and unbounded distributed delays based on sampled-data control is investigated. Lyapunov-Krasovskii functional combining with the input delay approach as well as the free-weighting matrix approach are employed to derive several sufficient criteria in terms of LMIs ensuring the delayed FCNNs to be asymptotically synchronous. The restriction such as the time-varying delay required to be differentiable or even its time-derivative assumed to be smaller than one, are removed. Instead, the time-varying delay is only assumed to be bounded. Finally, numerical examples and its simulations are provided to demonstrate the effectiveness of the derived results.

1. Introduction

Cellular neural networks (CNNs) are locally connected nonlinear networks. They originally stemmed from cellular automata and artificial neural networks (ANNs). Local connectedness is the most significant property of CNN. Continuous dynamics distinguish CNN from cellular automata. The local connectedness restricts the ability of CNN to solve many global problems that cannot be decomposed into local components. However, the local property has its advantages, such as easy implementation using VLSI technology and efficiency for solving local problems. CNNs were first introduced in twin papers by Chua and Yang (1988) [6, 7].

Fuzzy set theory provides an inference methodology that approximates human reasoning capabilities and can be applied to knowledge-based systems [36]. It provides mathematical support to the capture of uncertainties associated with human cognitive processes, for example, thinking and reasoning. Also, it provides a mathematical methodology to model linguistic statements and knowledge. FCNN is a generalized case of the CNN structure. FCNNs introduced by Yang et al. [32, 33], is proved to be a useful tool in image processing and pattern recognition [9, 31].

Consider the linear system

$$\dot{x}(t) = Ax(t), \qquad (1)$$

where $A \in \mathbb{R}^{n \times n}$ and $x(t) \in \mathbb{R}^n$. Assume that (1) has equilibrium $x^* = 0$.

Definition 1.1. Let $V : \mathbb{R}^n \to \mathbb{R}$ is a Lyapunov function for (1) if

    (i) $V(x(t)) \geq 0$ with equality if and only if $x^* = 0$, and

    (ii) $\dot{V}(x(t)) \leq 0$.

This leads to the celebrated theorem of Lyapunov of (1).

Theorem 1.2. *(Lyapunov's Second Theorem on $\mathbb{R}$) Given system (1) with equilibrium $x^* = 0$, if there exists an associated Lyapunov function V, then $x^* = 0$ is Lyapunov stable. Furthermore, if $\dot{V}(x(t)) < 0$, then $x^* = 0$ is asymptotically stable.*

The power of Theorem 1.2 is that one can make conclusions about trajectories of a system (1) without actually solving the differential equation. For the system (1), a common choice of Lyapunov function candidate is the quadratic form,

$$V(x(t)) = x^T(t)Px(t).$$

Investigating the stability of (1) is considering the time derivative of $V(x(t))$

$$
\begin{aligned}
\dot{V}(x(t)) &= x^T(t)P\dot{x}(t) + \dot{x}^T(t)Px(t) \\
&= x^T(t)PAx(t) + x^T(t)A^T Px(t) \\
&= x^T(t)\Big[PA + A^T P\Big]x(t).
\end{aligned}
$$

The quadratic form of this derivative proves, if the central quantity satisfies

$$PA + A^T P < 0,$$

then

$$\dot{V}(x(t)) < 0.$$

Example 1.3. Consider the linear system

$$\dot{x}(t) = \begin{bmatrix} -1 & 0 \\ 0 & -2 \end{bmatrix} x(t).$$

Using Matlab LMI control toolbox and solving the above LMI $PA + A^T P < 0$, one can get the following positive definite matrix $P = \begin{bmatrix} 1.1956 & 0 \\ 0 & 0.5861 \end{bmatrix}$. For this P, $PA + A^T P = \begin{bmatrix} -2.3912 & 0 \\ 0 & -2.3443 \end{bmatrix}$, which is negative definite. This implies that the given system is asymptotically stable in the sense of Lyapunov.

It is well known that time-delay is usually a cause of instability and oscillations of recurrent neural networks (RNNs). Therefore, the problem of stability of RNNs with time-delay is of importance in both theory and practical applications. With the help of the LMI approach, a number of research works have been devoted to analysis and synthesis of RNNs with various types of delays, such as stability analysis [2, 20, 25], and state estimation [1, 21].

Chaos has long-term unpredictable behavior. This is usually couched mathematically as sensitivity to initial conditions-where the system's dynamics takes it is

hard to predict from the starting point. Although a chaotic system can have a pattern (an attractor) in state space, determining where on the attractor the system is at a distant, future time given its position in the past is a problem that becomes exponentially harder as time passes [23]. One way to demonstrate this is to run, two identical chaotic systems side by side, starting both at close, but not exactly equal initial conditions. The systems soon diverge from each other, but both retain the same attractor pattern. That is, each has its own attractor without having any relation to the other system. It is possible to force the two chaotic systems to follow the same path on the attractor, namely synchronization. Carroll and Pecora [5, 22] have introduced the drive-response concept, and used the output of the drive system to control the response system to achieve the state synchronization.

Many results on synchronization of FCNNs with time-delays can be found in the literature [3, 12, 13, 24, 34, 35]. The controllers used for controlling and synchronizing chaos in continuous-time systems can be implemented by analog circuits. However, in order to take advantage of the modern high-speed computers, microelectronics, and communication networks, it is more preferable to use digital controllers instead of analog circuits, particularly in aerospace systems and industries [10, 11, 15, 17, 19, 37]. It allows synchronization of chaotic systems using the samples of the state variables of the master and the slave chaotic system at discrete time instants. These samples are used by sampled-data controllers to control the slave chaotic system and result in synchronization between the master and the slave chaotic systems [19]. This drastically reduces the amount of synchronization information transmitted from the master chaotic system to the slave chaotic system and increase the efficiency of bandwidth usage, which makes this method more efficient.
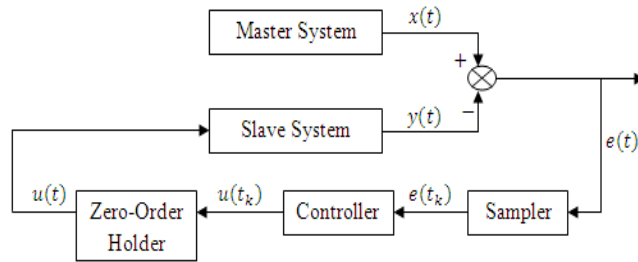

FIGURE 1. Block Diagram of Master-slave FCNNs with a Sampled-data Controller

In many real-world applications, it is difficult to guarantee that the state variables transmitted to controllers are continuous. In addition, in order to make full use of modern computer technique, the sampled-data feedback control is applied to synchronize delayed FCNNs. The block diagram of master-slave FCNNs with a sampling controller is shown in Figure 1. Referring to this Figure 1, the operation of this closed-system can be described as follows: Firstly, the system states of both the master and slave systems form error signal, which is fed to the sampler with a sampling interval, Δ_k. Then, the sampled system states information is processed by the sampled-data controller to produce an appropriate control signal. Finally, the control signal is kept constant during the sampling interval by the zero-order holder

and fed to the slave system to realize the synchronization. Moreover, the contribution of this paper is that we have compared our proposed results with the existing literature [3] and shown in Example 4.3 along with numerical simulations (Figures 13-14) and Table 1. However, to the best of authors' knowledge, the results on LMI approach for synchronization of chaotic FCNNs with discrete and unbounded distributed delays based on sampled-data control has never been investigated yet.

Motivated by the aforementioned discussions, in this paper, we derive new criteria for the synchronization of chaotic FCNNs based on sampled-data control, Lyapunov-Krasovskii functional, free-weighting matrix approach and LMI technique. Finally, two numerical examples and its simulations are given to show the effectiveness of proposed method.

Notations: $\mathbb{R}^n$ denotes the n-dimensional Euclidean Space; for any matrix $A = [a_{ij}]_{n \times n}$, let A^T and A^{-1} denote the transpose and the inverse of A, respectively; $|A| = [|a_{ij}|]_{n \times n}$; let $A > 0$ $(A < 0)$ denotes the positive-definite (negative-definite) symmetric matrix, respectively; the notation $\mathcal{C}^{2,1}(\mathbb{R}^+ \times \mathbb{R}^n; \mathbb{R}^+)$ denotes the family of all nonnegative functions $V(t, x(t))$ on $\mathbb{R}^+ \times \mathbb{R}^n$ which are continuously twice differentiable in x and once differentiable in t; I denotes the identity matrix of appropriate dimension and $\Lambda = \{1, 2, ..., n\}$; $\star$ denotes the symmetric terms in a symmetric matrix.

2. Model Formulation and Preliminaries

Consider the following general drive-response type chaotic FCNNs with discrete and unbounded distributed delays

$$\begin{cases} \dot{x}_i(t) = -d_i x_i(t) + \sum_{j=1}^n a_{ij} f_j(x_j(t)) + \sum_{j=1}^n b_{ij} f_j(x_j(t - \tau_1(t))) + I_i \\ \qquad + \bigwedge_{j=1}^n \alpha_{ij} \int_{-\infty}^t k_j(t-s) f_j(x_j(s)) ds \\ \qquad + \bigvee_{j=1}^n \beta_{ij} \int_{-\infty}^t k_j(t-s) f_j(x_j(s)) ds, \quad i \in \Lambda, \\ x_i(s) = \phi_i(s), \quad s \in (-\infty, 0], \end{cases} \quad (2)$$

and

$$\begin{cases} \dot{y}_i(t) = -d_i y_i(t) + \sum_{j=1}^n a_{ij} f_j(y_j(t)) + \sum_{j=1}^n b_{ij} f_j(y_j(t - \tau_1(t))) + I_i \\ \qquad + \bigwedge_{j=1}^n \alpha_{ij} \int_{-\infty}^t k_j(t-s) f_j(y_j(s)) ds \\ \qquad + \bigvee_{j=1}^n \beta_{ij} \int_{-\infty}^t k_j(t-s) f_j(y_j(s)) ds + u_i(t), \quad i \in \Lambda, \\ y_i(s) = \varphi_i(s), \quad s \in (-\infty, 0], \end{cases} \quad (3)$$

where $\phi_i(\cdot) \in C((-\infty, 0], \mathbb{R})$ and $\varphi_i(\cdot) \in C((-\infty, 0], \mathbb{R})$ are the initial conditions in drive system (2) and response system (3), respectively; α_{ij} and β_{ij} are the elements of fuzzy feedback MIN template and fuzzy feedback MAX template, respectively; a_{ij} and b_{ij} are the elements of feedback template; $\bigwedge$ and $\bigvee$ denote the fuzzy AND and fuzzy OR operation, respectively; x_i and y_i denote the state vectors in drive system (2) and response system (3) of the ith neuron, respectively; I_i denotes the external input of the ith neuron; d_i is a diagonal matrix, d_i represents the rates with which the ith neuron will reset their potential to the resting state in isolation when disconnected from the networks and external inputs; f_j represents the neuron activation function; $u(t) = (u_1(t), u_2(t), ..., u_n(t))^T$ is a control input to be designed.

$k_j(s) \geq 0$ is the feedback kernel and satisfies

$$\int_0^\infty k_i(s)ds = 1, \ i \in \Lambda. \tag{4}$$

Let $e(t) = \big(e_1(t), e_2(t), ..., e_n(t)\big) := x(t) - y(t)$ be the error state. Then, the error dynamical system between (2) and (3) is given by

$$\begin{cases} \dot{e}_i(t) = -d_i e_i(t) + \sum_{j=1}^n a_{ij} g_j(e_j(t)) + \sum_{j=1}^n b_{ij} g_j(e_j(t - \tau_1(t))) \\ \quad + \bigwedge_{j=1}^n \alpha_{ij} \int_{-\infty}^t k_j(t-s) f_j(x_j(s)) ds - \bigwedge_{j=1}^n \alpha_{ij} \int_{-\infty}^t k_j(t-s) f_j(y_j(s)) ds \\ \quad + \bigvee_{j=1}^n \beta_{ij} \int_{-\infty}^t k_j(t-s) f_j(x_j(s)) ds - \bigvee_{j=1}^n \beta_{ij} \int_{-\infty}^t k_j(t-s) f_j(y_j(s)) ds \\ \quad - u_i(t), \quad i \in \Lambda, \\ e_i(s) = \phi_i(s) - \varphi_i(s) = \psi_i(s), \quad s \in (-\infty, 0], \end{cases} \tag{5}$$

where $g_j(e_j(\cdot)) = f_j(x_j(\cdot)) - f_j(y_j(\cdot)), \ j \in \Lambda$.

The sampled-data control law can be adopted as follows:

$$u_i(t) := h_{ij} e_i(t_k), \ t_k \leq t < t_{k+1}, \quad i, j \in \Lambda, \tag{6}$$

where h_{ij} is the element of sampled-data feedback controller gain matrix to be determined, $e(t_k)$ is discrete measurement of $e(t)$ at the sampling instant t_k; and t_k satisfies the following conditions:

$$0 = t_0 < t_1 < t_2 < ... < t_k < ... < \lim_{k \to +\infty} t_k = +\infty.$$

Moreover, the sampling period under consideration is assumed to be bounded by a known constant τ_2, that is, $\Delta_k = t_{k+1} - t_k \leq \tau_2$ for $k \geq 0$.

Substituting control law (6) into the error system (5) yields,

$$\begin{cases} \dot{e}_i(t) = -d_i e_i(t) + \sum_{j=1}^n a_{ij} g_j(e_j(t)) + \sum_{j=1}^n b_{ij} g_j(e_j(t - \tau_1(t))) \\ \quad + \bigwedge_{j=1}^n \alpha_{ij} \int_{-\infty}^t k_j(t-s) f_j(x_j(s)) ds - \bigwedge_{j=1}^n \alpha_{ij} \int_{-\infty}^t k_j(t-s) f_j(y_j(s)) ds \\ \quad + \bigvee_{j=1}^n \beta_{ij} \int_{-\infty}^t k_j(t-s) f_j(x_j(s)) ds - \bigvee_{j=1}^n \beta_{ij} \int_{-\infty}^t k_j(t-s) f_j(y_j(s)) ds \\ \quad - h_{ij} e_i(t_k), \quad i \in \Lambda, \\ e_i(s) = \psi_i(s), \quad s \in (-\infty, 0]. \end{cases} \tag{7}$$

Clearly, it is difficult to analyze the synchronization of chaotic FCNNs based on error system (7) because of the discrete term, $e(t_k)$. Therefore, the input delay approach [10] is applied, by defining

$$\tau_2(t) = t - t_k, \quad t_k \leq t < t_{k+1}. \tag{8}$$

It is easily seen that

$$0 \leq \tau_2(t) < \tau_2. \tag{9}$$

Therefore, the state-feedback controller takes the following form

$$u_i(t) = h_{ij} e_i(t - \tau_2(t)), \ t_k \leq t < t_{k+1}, \quad i, j \in \Lambda. \tag{10}$$

Consequently, connecting (10) to system (7) yields

$$\begin{cases} \dot{e}_i(t) = -d_i e_i(t) + \sum_{j=1}^n a_{ij} g_j(e_j(t)) + \sum_{j=1}^n b_{ij} g_j(e_j(t - \tau_1(t))) \\ \quad + \bigwedge_{j=1}^n \alpha_{ij} \int_{-\infty}^t k_j(t-s) f_j(x_j(s)) ds - \bigwedge_{j=1}^n \alpha_{ij} \int_{-\infty}^t k_j(t-s) f_j(y_j(s)) ds \\ \quad + \bigvee_{j=1}^n \beta_{ij} \int_{-\infty}^t k_j(t-s) f_j(x_j(s)) ds - \bigvee_{j=1}^n \beta_{ij} \int_{-\infty}^t k_j(t-s) f_j(y_j(s)) ds \\ \quad - h_{ij} e_i(t - \tau_2(t)), \quad i \in \Lambda, \\ e_i(s) = \psi_i(s), \quad s \in (-\infty, 0]. \end{cases} \tag{11}$$

We list two assumptions as follows:

(A_1) The neuron activation function $f_j(\cdot)$, $j \in \Lambda$, are continuously bounded and satisfies
$$l_j^- \leq \frac{f_j(u) - f_j(v)}{u - v} \leq l_j^+, \text{ for any } u, \ v \in \mathbb{R}, \ u \neq v, \ j \in \Lambda,$$
where l_j^- and l_j^+ are some real constants and they may be positive, zero or negative.

(A_2) The transmission delay $\tau_1(t)$ is a time varying delay, and it satisfies $0 \leq \tau_1(t) \leq \tau_1$, where τ_1 is a positive constant.

We state the following lemmas which will be used in the sequel to prove the main result.

Lemma 2.1. *(Schur Complement [4]) The LMI* $\begin{bmatrix} Q(x) & S(x) \\ S^T(x) & R(x) \end{bmatrix} > 0$, *where* $Q(x) = Q^T(x)$, $R(x) = R^T(x)$, *is equivalent to*
$$R(x) > 0 \text{ and } Q(x) - S(x)R^{-1}(x)S^T(x) > 0.$$

Lemma 2.2. *[26] For any $x, y \in \mathbb{R}^n$, $\epsilon > 0$ and positive definite matrix $Q \in \mathbb{R}^{n \times n}$, the following matrix inequality holds*
$$2x^T y \leq \epsilon x^T Q x + \epsilon^{-1} y^T Q^{-1} y.$$

Lemma 2.3. *[31] Let z, z' be two states of system (2), then we have*
$$| \bigwedge_{j=1}^n \alpha_{ij} f_j(z) - \bigwedge_{j=1}^n \alpha_{ij} f_j(z') | \leq \sum_{j=1}^n |\alpha_{ij}| |f_j(z) - f_j(z')|,$$
$$| \bigvee_{j=1}^n \beta_{ij} f_j(z) - \bigvee_{j=1}^n \beta_{ij} f_j(z') | \leq \sum_{j=1}^n |\beta_{ij}| |f_j(z) - f_j(z')|.$$

Lemma 2.4. *[18] For any $x \in \mathbb{R}^n$, any constant matrix $A = [a_{ij}]_{n \times n}$ with $a_{ij} \geq 0$, the following matrix inequality holds*
$$x^T A^T A x \leq n x^T A_s^T A_s x,$$
where $A_s = diag\Big\{ \sum_{i=1}^n a_{i1}, \sum_{i=1}^n a_{i2}, ..., \sum_{i=1}^n a_{in} \Big\}$.

Lemma 2.5. *[14] Given any real matrix $M = M^T > 0$ of appropriate dimension, and a vector function $\omega(\cdot) : [a, b] \to \mathbb{R}^n$, such that the integrations concerned are well defined, then*
$$\Big[\int_a^b \omega(s) ds \Big]^T M \Big[\int_a^b \omega(s) ds \Big] \leq (b - a) \int_a^b \omega^T(s) M \omega(s) ds.$$

The main purpose of this paper is to design controller with the form (10) to ensure the master system (2) synchronize with slave system (3). In other words, we are interested in finding a feedback gain matrix H such that the error system (11) is asymptotically stable.

3. Main Results

Theorem 3.1. *Assume that assumptions $(A_1) - (A_2)$ hold. The error dynamical system (11) is globally asymptotically stable, if there exist $n \times n$ positive diagonal matrices P, R, U_1, U_2, U_3, some $n \times n$ positive definite symmetric matrices*

Q_0, Q_1, Q_2, W_1, W_2, M_1, M_2, M_3, M_4, *some positive scalars* μ_1, μ_2 *and the* $2n \times 2n$ *matrices* $\begin{pmatrix} T_{11} & T_{12} \\ \star & T_{22} \end{pmatrix} > 0$, $\begin{pmatrix} V_{11} & V_{12} \\ \star & V_{22} \end{pmatrix} > 0$, *such that the following LMI has feasible solution:*

$$\Omega = \begin{bmatrix} \Omega_{i,j} & \Gamma_1^T & \Gamma_2^T \\ \star & -\mu_1 n^{-1}I & 0 \\ \star & \star & -\mu_2 n^{-1}I \end{bmatrix} < 0, \tag{12}$$

where $i, j = 1, 2, ..., 16$ *with*

$$\Omega_{1,1} = -2PD + Q_1 + Q_2 - \frac{1}{\tau_1}M_1 - \frac{1}{\tau_2}M_2 - 2M_3 - 2M_4 - U_1\Sigma_1,$$

$$\Omega_{1,2} = \frac{1}{\tau_1}M_1, \Omega_{1,3} = T_{12}^T, \Omega_{1,4} = \frac{1}{\tau_2}M_2, \Omega_{1,5} = -Q_0 + V_{12}^T, \Omega_{1,6} = -D^T P,$$

$$\Omega_{1,9} = \frac{2}{\tau_1}M_3, \Omega_{1,10} = \frac{2}{\tau_1}M_3, \Omega_{1,11} = \frac{2}{\tau_2}M_4, \Omega_{1,12} = \frac{2}{\tau_2}M_4, \Omega_{1,13} = PA + U_1\Sigma_2,$$

$$\Omega_{1,14} = PB, \Omega_{2,2} = -Q_1 - \frac{1}{\tau_1}M_1, \Omega_{3,3} = \tau_1 T_{11} - 2T_{12}^T - U_2\Sigma_1, \Omega_{3,14} = U_2\Sigma_2,$$

$$\Omega_{4,4} = -Q_2 - \frac{1}{\tau_2}M_2, \Omega_{5,5} = \tau_2 V_{11} - 2V_{12}^T - U_3\Sigma_1, \Omega_{5,6} = -Q_0^T, \Omega_{5,15} = U_3\Sigma_2,$$

$$\Omega_{6,6} = -2P + W_1 + W_2 + \tau_1 M_1 + \tau_2 M_2 + \frac{\tau_1^2}{2}M_3 + \frac{\tau_2^2}{2}M_4 + \tau_1 T_{22} + \tau_2 V_{22},$$

$$\Omega_{6,13} = PA, \ \Omega_{6,14} = PB, \ \Omega_{7,7} = -W_1, \ \Omega_{8,8} = -W_2, \ \Omega_{9,9} = -\frac{2}{\tau_1^2}M_3,$$

$$\Omega_{9,10} = -\frac{2}{\tau_1^2}M_3, \ \Omega_{10,10} = -\frac{2}{\tau_1^2}M_3, \ \Omega_{11,11} = -\frac{2}{\tau_2^2}M_4, \ \Omega_{11,12} = -\frac{2}{\tau_2^2}M_4,$$

$$\Omega_{12,12} = -\frac{2}{\tau_2^2}M_4, \ \Omega_{13,13} = R - U_1, \ \Omega_{14,14} = -U_2, \ \Omega_{15,15} = -U_3,$$

$$\Omega_{16,16} = \mu_1 I + \mu_2 I - R, \ |\alpha|_s = diag\left\{\sum_{i=1}^{n}|\alpha_{i1}|, \sum_{i=1}^{n}|\alpha_{i2}|, ..., \sum_{i=1}^{n}|\alpha_{in}|\right\},$$

$$|\beta|_s = diag\left\{\sum_{i=1}^{n}|\beta_{i1}|, \sum_{i=1}^{n}|\beta_{i2}|, ..., \sum_{i=1}^{n}|\beta_{in}|\right\}, \ S = |\alpha|_s + |\beta|_s,$$

$$\Sigma_1 = diag\left\{l_1^- l_1^+, ..., l_n^- l_n^+\right\}, \ \Sigma_2 = diag\left\{\frac{l_1^- + l_1^+}{2}, ..., \frac{l_n^- + l_n^+}{2}\right\},$$

$$\Gamma_1^T = \begin{bmatrix} PS & 0 & 0 & 0 & 0 & 0 & 0 & 0 & 0 & 0 & 0 & 0 & 0 & 0 & 0 & 0 \end{bmatrix}^T,$$

$$\Gamma_2^T = \begin{bmatrix} 0 & 0 & 0 & 0 & 0 & PS & 0 & 0 & 0 & 0 & 0 & 0 & 0 & 0 & 0 & 0 \end{bmatrix}^T.$$

Moreover, the controller gain matrix $H = P^{-1}Q_0$.

Proof. Consider the following Lyapunov-Krasovskii functional

$$V(t) = \sum_{i=1}^{7} V_i(t), \tag{13}$$

where

$$V_1(t) = e^T(t)Pe(t) = \sum_{i=1}^{n} p_i e_i^2(t),$$

$$V_2(t) = \int_{t-\tau_1}^{t} e^T(s)Q_1 e(s)ds + \int_{t-\tau_2}^{t} e^T(s)Q_2 e(s)ds$$
$$+ \int_{t-\tau_1}^{t} \dot{e}^T(s)W_1\dot{e}(s)ds + \int_{t-\tau_2}^{t} \dot{e}^T(s)W_2\dot{e}(s)ds,$$

$$V_3(t) = \sum_{j=1}^{n} r_j \int_{0}^{\infty} k_j(\theta) \int_{t-\theta}^{t} g_j^2(e_j(s))dsd\theta,$$

$$V_4(t) = \int_{-\tau_1}^{0} \int_{t+\theta}^{t} \dot{e}^T(s)M_1\dot{e}(s)dsd\theta + \int_{-\tau_2}^{0} \int_{t+\theta}^{t} \dot{e}^T(s)M_2\dot{e}(s)dsd\theta,$$

$$V_5(t) = \int_{-\tau_1}^{0} \int_{\theta}^{0} \int_{t+\lambda}^{t} \dot{e}^T(s)M_3\dot{e}(s)dsd\lambda d\theta + \int_{-\tau_2}^{0} \int_{\theta}^{0} \int_{t+\lambda}^{t} \dot{e}^T(s)M_4\dot{e}(s)dsd\lambda d\theta,$$

$$V_6(t) = \int_{0}^{t} \int_{\theta-\tau_1(\theta)}^{\theta} \begin{bmatrix} e(\theta-\tau_1(\theta)) \\ \dot{e}(s) \end{bmatrix}^T \begin{bmatrix} T_{11} & T_{12} \\ \star & T_{22} \end{bmatrix} \begin{bmatrix} e(\theta-\tau_1(\theta)) \\ \dot{e}(s) \end{bmatrix} dsd\theta$$
$$+ \int_{0}^{t} \int_{\theta-\tau_2(\theta)}^{\theta} \begin{bmatrix} e(\theta-\tau_2(\theta)) \\ \dot{e}(s) \end{bmatrix}^T \begin{bmatrix} V_{11} & V_{12} \\ \star & V_{22} \end{bmatrix} \begin{bmatrix} e(\theta-\tau_2(\theta)) \\ \dot{e}(s) \end{bmatrix} dsd\theta,$$

$$V_7(t) = \int_{-\tau_1}^{0} \int_{t+\theta}^{t} \dot{e}^T(s)T_{22}\dot{e}(s)dsd\theta + \int_{-\tau_2}^{0} \int_{t+\theta}^{t} \dot{e}^T(s)V_{22}\dot{e}(s)dsd\theta.$$

From Lemma 2.3, we obtain

$$\Big| \bigwedge_{j=1}^{n} \alpha_{ij} \int_{-\infty}^{t} k_j(t-s)f_j(x_j)ds - \bigwedge_{j=1}^{n} \alpha_{ij} \int_{-\infty}^{t} k_j(t-s)f_j(y_j)ds \Big|$$
$$\leq \sum_{j=1}^{n} |\alpha_{ij}| \Big| \int_{-\infty}^{t} k_j(t-s)g_j(e_j(s))ds \Big|.$$

By calculating the time derivation of $V_i(t)$ along the trajectory of system (11), we obtain

$$\begin{aligned}
\dot{V}_1(t) \leq & -2e^T(t)PDe(t) - 2e^T(t)Q_0 e(t-\tau_2(t)) + 2e^T(t)PAg(e(t)) + 2e^T(t)PB \\
& \times g(e(t-\tau_1(t))) + \mu_1^{-1}ne^T(t)P\,(|\alpha|_s + |\beta|_s)(|\alpha|_s + |\beta|_s)^T Pe(t) \\
& + \mu_1 \Big(\int_{-\infty}^{t} K(t-s)g(e(s))ds \Big)^T \Big(\int_{-\infty}^{t} K(t-s)g(e(s))ds \Big) \\
& -2\dot{e}^T(t)P\dot{e}(t) - 2\dot{e}^T(t)PDe(t) + 2\dot{e}^T(t)PAg(e(t)) + 2\dot{e}^T(t)PB \\
& \times g(e(t-\tau_1(t))) + \mu_2^{-1}n\dot{e}^T(t)P(|\alpha|_s + |\beta|_s)(|\alpha|_s + |\beta|_s)^T P\dot{e}(t) \\
& + \mu_2 \Big(\int_{-\infty}^{t} K(t-s)g(e(s))ds \Big)^T \Big(\int_{-\infty}^{t} K(t-s)g(e(s))ds \Big) \\
& -2\dot{e}^T(t)Q_0 e(t-\tau_2(t)),
\end{aligned}$$

$$(14)$$

$$
\begin{aligned}
\dot{V}_2(t) \;=\; & e^T(t)Q_1 e(t) - e^T(t-\tau_1)Q_1 e(t-\tau_1) + e^T(t)Q_2 e(t) \\
& -e^T(t-\tau_2)Q_2 e(t-\tau_2) + \dot{e}^T(t)W_1 \dot{e}(t) - \dot{e}^T(t-\tau_1)W_1 \dot{e}(t-\tau_1) \\
& +\dot{e}^T(t)W_2 \dot{e}(t) - \dot{e}^T(t-\tau_2)W_2 \dot{e}(t-\tau_2),
\end{aligned} \tag{15}
$$

$$
\begin{aligned}
\dot{V}_3(t) \;=\; & g^T(e(t))Rg(e(t)) - \sum_{j=1}^{n} r_j \Big(\int_0^\infty k_j(\theta) g_j(e_j(t-\theta))d\theta \Big)^2 \\
\;=\; & g^T(e(t))Rg(e(t)) - \Big(\int_{-\infty}^{t} K(t-s)g(e(s))ds \Big)^T R \Big(\int_{-\infty}^{t} K(t-s) \\
& \times g(e(s))ds \Big),
\end{aligned} \tag{16}
$$

$$
\begin{aligned}
\dot{V}_4(t) \;\le\; & \tau_1 \dot{e}^T(t)M_1 \dot{e}(t) - \frac{1}{\tau_1} e^T(t)M_1 e(t) + \frac{2}{\tau_1} e^T(t)M_1 e(t-\tau_1) \\
& -\frac{1}{\tau_1} e^T(t-\tau_1)M_1 e(t-\tau_1) + \tau_2 \dot{e}^T(t)M_2 \dot{e}(t) - \frac{1}{\tau_2} e^T(t)M_2 e(t) + \frac{2}{\tau_2} \\
& \times e^T(t)M_2 e(t-\tau_2) - \frac{1}{\tau_2} e^T(t-\tau_2)M_2 e(t-\tau_2),
\end{aligned} \tag{17}
$$

$$
\begin{aligned}
\dot{V}_5(t) \;\le\; & \frac{\tau_1^2}{2} \dot{e}^T(t)M_3 \dot{e}(t) - 2e^T(t)M_3 e(t) + \frac{2}{\tau_1} e^T(t)M_3 \int_{t-\tau_1(t)}^{t} e(s)ds \\
& +\frac{2}{\tau_1} e^T(t)M_3 \int_{t-\tau_1}^{t-\tau_1(t)} e(s)ds + \frac{2}{\tau_1} \int_{t-\tau_1(t)}^{t} e^T(s)ds M_3 e(t) \\
& -\frac{2}{\tau_1^2} \int_{t-\tau_1(t)}^{t} e^T(s)ds \, M_3 \int_{t-\tau_1(t)}^{t} e(s)ds - \frac{2}{\tau_1^2} \int_{t-\tau_1(t)}^{t} e^T(s)ds M_3 \\
& \times \int_{t-\tau_1}^{t-\tau_1(t)} e(s)ds + \frac{2}{\tau_1} \int_{t-\tau_1}^{t-\tau_1(t)} e^T(s)ds M_3 e(t) - \frac{2}{\tau_1^2} \int_{t-\tau_1}^{t-\tau_1(t)} e^T(s)ds \\
& \times M_3 \int_{t-\tau_1(t)}^{t} e(s)ds - \frac{2}{\tau_1^2} \int_{t-\tau_1}^{t-\tau_1(t)} e^T(s)ds \, M_3 \int_{t-\tau_1}^{t-\tau_1(t)} e(s)ds \\
& +\frac{\tau_2^2}{2} \dot{e}^T(t)M_4 \dot{e}(t) - 2e^T(t)M_4 e(t) + \frac{2}{\tau_2} e^T(t)M_4 \int_{t-\tau_2(t)}^{t} e(s)ds \\
& +\frac{2}{\tau_2} e^T(t)M_4 \int_{t-\tau_2}^{t-\tau_2(t)} e(s)ds + \frac{2}{\tau_2} \int_{t-\tau_2(t)}^{t} e^T(s)ds M_4 e(t) \\
& -\frac{2}{\tau_2^2} \int_{t-\tau_2(t)}^{t} e^T(s)ds \, M_4 \int_{t-\tau_2(t)}^{t} e(s)ds - \frac{2}{\tau_2^2} \int_{t-\tau_2(t)}^{t} e^T(s)ds M_4 \\
& \times \int_{t-\tau_2}^{t-\tau_2(t)} e(s)ds + \frac{2}{\tau_2} \int_{t-\tau_2}^{t-\tau_2(t)} e^T(s)ds \, M_4 e(t) - \frac{2}{\tau_2^2} \int_{t-\tau_2}^{t-\tau_2(t)} e^T(s)ds \\
& \times M_4 \int_{t-\tau_2(t)}^{t} e(s)ds - \frac{2}{\tau_2^2} \int_{t-\tau_2}^{t-\tau_2(t)} e^T(s)ds \, M_4 \int_{t-\tau_2}^{t-\tau_2(t)} e(s)ds,
\end{aligned} \tag{18}
$$

$$
\begin{aligned}
\dot{V}_6(t) \;\le\; & e^T(t-\tau_1(t))\Big[\tau_1 T_{11} - 2T_{12}^T\Big]e(t-\tau_1(t)) + 2e^T(t)T_{12}^T e(t-\tau_1(t)) \\
& + \int_{t-\tau_1}^t \dot{e}^T(s)T_{22}\dot{e}(s)ds + e^T(t-\tau_2(t))\Big[\tau_2 V_{11} - 2V_{12}^T\Big]e(t-\tau_2(t)) \\
& + 2e^T(t)V_{12}^T e(t-\tau_2(t)) + \int_{t-\tau_2}^t \dot{e}^T(s)V_{22}\dot{e}(s)ds,
\end{aligned}
\tag{19}
$$

$$
\begin{aligned}
\dot{V}_7(t) \;=\; & \tau_1 \dot{e}^T(t)T_{22}\dot{e}(t) - \int_{-\tau_1}^0 \dot{e}^T(t+\theta)T_{22}\dot{e}(t+\theta)d\theta + \tau_2 \dot{e}^T(t)V_{22}\dot{e}(t) \\
& - \int_{-\tau_2}^0 \dot{e}^T(t+\theta)V_{22}\dot{e}(t+\theta)d\theta \\
\;=\; & \tau_1 \dot{e}^T(t)T_{22}\dot{e}(t) - \int_{t-\tau_1}^t \dot{e}^T(s)T_{22}\dot{e}(s)ds \\
& + \tau_2 \dot{e}^T(t)V_{22}\dot{e}(t) - \int_{t-\tau_2}^t \dot{e}^T(s)V_{22}\dot{e}(s)ds.
\end{aligned}
\tag{20}
$$

In addition, for any $n \times n$ diagonal matrices $U_1 > 0$, $U_2 > 0$, $U_3 > 0$, the following inequality holds by the methods proposed in [16]:

$$
\begin{aligned}
\Bigg\{ & \begin{bmatrix} e(t) \\ g(e(t)) \end{bmatrix}^T \begin{bmatrix} -U_1\Sigma_1 & U_1\Sigma_2 \\ \star & -U_1 \end{bmatrix} \begin{bmatrix} e(t) \\ g(e(t)) \end{bmatrix} \\
& + \begin{bmatrix} e(t-\tau_1(t)) \\ g(e(t-\tau_1(t))) \end{bmatrix}^T \begin{bmatrix} -U_2\Sigma_1 & U_2\Sigma_2 \\ \star & -U_2 \end{bmatrix} \begin{bmatrix} e(t-\tau_1(t)) \\ g(e(t-\tau_1(t))) \end{bmatrix} \\
& + \begin{bmatrix} e(t-\tau_2(t)) \\ g(e(t-\tau_2(t))) \end{bmatrix}^T \begin{bmatrix} -U_3\Sigma_1 & U_3\Sigma_2 \\ \star & -U_3 \end{bmatrix} \begin{bmatrix} e(t-\tau_2(t)) \\ g(e(t-\tau_2(t))) \end{bmatrix} \Bigg\} \ge 0.
\end{aligned}
\tag{21}
$$

Hence, from (13)-(21) we have

$$
\begin{aligned}
\dot{V}(t) \;\le\; & \xi^T(t)\left[\Omega_{i,j} + \Gamma_1^T \mu_1^{-1} n\Gamma_1 + \Gamma_2^T \mu_2^{-1} n\Gamma_2\right]\xi(t) \\
\;=\; & \xi^T(t)\,\Omega\,\xi(t),
\end{aligned}
\tag{22}
$$

where

$$
\begin{aligned}
\xi(t) \;=\; & \Big[e^T(t),\; e^T(t-\tau_1),\; e^T(t-\tau_1(t)),\; e^T(t-\tau_2),\; e^T(t-\tau_2(t)),\; \dot{e}^T(t), \\
& \dot{e}^T(t-\tau_1),\; \dot{e}^T(t-\tau_2),\; \int_{t-\tau_1(t)}^t e^T(s)ds,\; \int_{t-\tau_1}^{t-\tau_1(t)} e^T(s)ds, \\
& \int_{t-\tau_2(t)}^t e^T(s)ds,\; \int_{t-\tau_2}^{t-\tau_2(t)} e^T(s)ds,\; g^T(e(t)),\; g^T(e(t-\tau_1(t))), \\
& g^T(e(t-\tau_2(t))),\; \int_{-\infty}^t K(t-s)g^T(e(s))ds \Big]^T, \\
\Omega \;=\; & \Omega_{i,j} + \Gamma_1^T \mu_1^{-1} n\Gamma_1 + \Gamma_2^T \mu_2^{-1} n\Gamma_2.
\end{aligned}
$$

By (12), it yields

$$\dot{V}(t) \quad \leq \quad -\xi^T(t)\,\Omega^\star\,\xi(t), \quad t > 0,$$

where $\Omega^\star = -\Omega > 0$. Therefore, we can conclude that the error dynamical system (11) is globally asymptotically stable. As a result, the slave chaotic FCNNs with discrete and unbounded distributed delays (3) is globally synchronized with the master FCNNs (2). This completes the proof. $\qquad\square$

Remark 3.2. The motivation for the use of null terms with the introduction of free-weighting matrices, when considering the stability analysis of neural networks has been investigated [27, 28, 29]. In Theorem 3.1, we have introduced the diagonal matrix P as free-weighting matrix by using the artifice: $-\dot{e}(t)+\dot{e}(t) = 0$. It is worth pointing out that the less free-weighting matrices method is regarded as an effective way to reduce the conservatism of the derived theoretical stability results. Note that the assumptions (A_1), (A_2) on activation function and time-varying delay in this paper are weaker than those generally used in the literature [8, 30]; namely, the boundedness of the activation function f_j. Further the differentiability of the time varying delay $\tau_1(t)$ is not required in this paper.

Remark 3.3. In the absence of unbounded distributed delay, the master FCNNs system (2) becomes as follows

$$\begin{cases} \dot{x}_i(t) = -d_i x_i(t) + \sum_{j=1}^n a_{ij} f_j(x_j(t)) + \sum_{j=1}^n b_{ij} f_j(x_j(t - \tau_1(t))) + I_i \\ \qquad + \bigwedge_{j=1}^n \alpha_{ij} f_j(x_j(t - \tau_1(t))) + \bigvee_{j=1}^n \beta_{ij} f_j(x_j(t - \tau_1(t))), \ i \in \Lambda, \\ x_i(s) = \phi_i(s), \quad s \in (-\infty, 0]. \end{cases} \quad (23)$$

and the corresponding response system of (23) is given by

$$\begin{cases} \dot{y}_i(t) = -d_i y_i(t) + \sum_{j=1}^n a_{ij} f_j(y_j(t)) + \sum_{j=1}^n b_{ij} f_j(y_j(t - \tau_1(t))) + I_i \\ \qquad + \bigwedge_{j=1}^n \alpha_{ij} f_j(y_j(t - \tau_1(t))) + \bigvee_{j=1}^n \beta_{ij} f_j(y_j(t - \tau_1(t))) + u_i(t), \ i \in \Lambda, \\ y_i(s) = \varphi_i(s), \quad s \in (-\infty, 0], \end{cases} \quad (24)$$

where $\phi_i(\cdot)$, $\varphi_i(\cdot)$, d_i, a_{ij}, b_{ij}, α_{ij}, β_{ij}, I_i, f_j and $u_i(t)$ described in (23) and (24) are the same as (2) and (3), respectively.

Let $e(t) = \big(e_1(t), e_2(t), ..., e_n(t)\big) := x(t) - y(t)$ be the error state. Then, the error dynamical system between (23) and (24) is given by

$$\begin{cases} \dot{e}_i(t) = -d_i e_i(t) + \sum_{j=1}^n a_{ij} g_j(e_j(t)) + \sum_{j=1}^n b_{ij} g_j(e_j(t - \tau_1(t))) \\ \qquad + \bigwedge_{j=1}^n \alpha_{ij} f_j(x_j(t - \tau_1(t))) - \bigwedge_{j=1}^n \alpha_{ij} f_j(y_j(t - \tau_1(t))) + \bigvee_{j=1}^n \beta_{ij} \\ \qquad \times f_j(x_j(t - \tau_1(t))) - \bigvee_{j=1}^n \beta_{ij} f_j(y_j(t - \tau_1(t))) - h_{ij} e_i(t - \tau_2(t)), \ i \in \Lambda, \\ e_i(s) = \phi_i(s) - \varphi_i(s) = \psi_i(s), \quad s \in (-\infty, 0], \end{cases} \quad (25)$$

where $g_j(e_j(\cdot)) = f_j(x_j(\cdot)) - f_j(y_j(\cdot))$, $j \in \Lambda$.

Moreover, the following Corollary 3.4 is a special case of Theorem 3.1.

Corollary 3.4. *Assume that assumptions $(A_1) - (A_2)$ hold. The error dynamical system (25) is globally asymptotically stable, if there exist $n \times n$ positive diagonal matrices P, U_1, U_2, U_3, some $n \times n$ positive definite symmetric matrices Q_0, Q_1, Q_2, W_1, W_2, M_1, M_2, M_3, M_4, a positive scalar μ, and the $2n \times 2n$*

matrices $\begin{pmatrix} T_{11} & T_{12} \\ \star & T_{22} \end{pmatrix} > 0,$ $\begin{pmatrix} V_{11} & V_{12} \\ \star & V_{22} \end{pmatrix} > 0,$ *such that the following LMI has feasible solution:*

$$\Omega = \begin{bmatrix} \Omega_{i,j} & \Gamma^T \\ \star & -\mu n^{-1}I \end{bmatrix} < 0, \tag{26}$$

where $i, j = 1, 2, ..., 15$ *with*

$$\Omega_{1,1} = -2PD + P + Q_1 + Q_2 - \frac{1}{\tau_1}M_1 - \frac{1}{\tau_2}M_2 - 2M_3 - 2M_4 - U_1\Sigma_1,$$

$$\Omega_{1,2} = \frac{1}{\tau_1}M_1, \Omega_{1,3} = T_{12}^T, \Omega_{1,4} = \frac{1}{\tau_2}M_2, \Omega_{1,5} = -Q_0 + V_{12}^T, \Omega_{1,6} = -D^T P,$$

$$\Omega_{1,9} = \frac{2}{\tau_1}M_3, \ \Omega_{1,10} = \frac{2}{\tau_1}M_3, \ \Omega_{1,11} = \frac{2}{\tau_2}M_4, \ \Omega_{1,12} = \frac{2}{\tau_2}M_4,$$

$$\Omega_{1,13} = PA + U_1\Sigma_2, \ \Omega_{1,14} = PB, \ \Omega_{2,2} = -Q_1 - \frac{1}{\tau_1}M_1,$$

$$\Omega_{3,3} = \tau_1 T_{11} - 2T_{12}^T - U_2\Sigma_1, \ \Omega_{3,14} = U_2\Sigma_2, \ \Omega_{4,4} = -Q_2 - \frac{1}{\tau_2}M_2,$$

$$\Omega_{5,5} = \tau_2 V_{11} - 2V_{12}^T - U_3\Sigma_1, \ \Omega_{5,6} = -Q_0^T, \ \Omega_{5,15} = U_3\Sigma_2,$$

$$\Omega_{6,6} = -2P + W_1 + W_2 + \tau_1 M_1 + \tau_2 M_2 + \frac{\tau_1^2}{2}M_3 + \frac{\tau_2^2}{2}M_4 + \tau_1 T_{22} + \tau_2 V_{22},$$

$$\Omega_{6,13} = PA, \ \Omega_{6,14} = PB, \ \Omega_{7,7} = -W_1, \ \Omega_{8,8} = -W_2, \ \Omega_{9,9} = -\frac{2}{\tau_1^2}M_3,$$

$$\Omega_{9,10} = -\frac{2}{\tau_1^2}M_3, \ \Omega_{10,10} = -\frac{2}{\tau_1^2}M_3, \ \Omega_{11,11} = -\frac{2}{\tau_2^2}M_4, \ \Omega_{11,12} = -\frac{2}{\tau_2^2}M_4,$$

$$\Omega_{12,12} = -\frac{2}{\tau_2^2}M_4, \ \Omega_{13,13} = -U_1, \ \Omega_{14,14} = nS^T PS + \mu I - U_2, \ \Omega_{15,15} = -U_3,$$

$$|\alpha|_s = diag\Big\{ \sum_{i=1}^n |\alpha_{i1}|, \sum_{i=1}^n |\alpha_{i2}|, ..., \sum_{i=1}^n |\alpha_{in}| \Big\},$$

$$|\beta|_s = diag\Big\{ \sum_{i=1}^n |\beta_{i1}|, \sum_{i=1}^n |\beta_{i2}|, ..., \sum_{i=1}^n |\beta_{in}| \Big\},$$

$$S = |\alpha|_s + |\beta|_s, \Sigma_1 = diag\Big\{ l_1^- l_1^+, ..., l_n^- l_n^+ \Big\}, \Sigma_2 = diag\Big\{ \frac{l_1^- + l_1^+}{2}, ..., \frac{l_n^- + l_n^+}{2} \Big\},$$

$$\Gamma^T = \begin{bmatrix} 0 & 0 & 0 & 0 & 0 & (PS)^T & 0 & 0 & 0 & 0 & 0 & 0 & 0 & 0 & 0 \end{bmatrix}^T.$$

Moreover, the controller gain matrix $H = P^{-1}Q_0$.

Proof. Consider the following Lyapunov-Krasovskii functional

$$V(t) = \sum_{i=1}^6 V_i(t), \tag{27}$$

where

$$V_1(t) = e^T(t)Pe(t)$$

$$V_2(t) = \int_{t-\tau_1}^t e^T(s)Q_1 e(s)ds + \int_{t-\tau_2}^t e^T(s)Q_2 e(s)ds$$

$$+ \int_{t-\tau_1}^t \dot{e}^T(s)W_1\dot{e}(s)ds + \int_{t-\tau_2}^t \dot{e}^T(s)W_2\dot{e}(s)ds,$$

$$V_3(t) = \int_{-\tau_1}^0 \int_{t+\theta}^t \dot{e}^T(s)M_1\dot{e}(s)dsd\theta + \int_{-\tau_2}^0 \int_{t+\theta}^t \dot{e}^T(s)M_2\dot{e}(s)dsd\theta,$$

$$V_4(t) = \int_{-\tau_1}^0 \int_\theta^0 \int_{t+\lambda}^t \dot{e}^T(s)M_3\dot{e}(s)dsd\lambda d\theta + \int_{-\tau_2}^0 \int_\theta^0 \int_{t+\lambda}^t \dot{e}^T(s)M_4\dot{e}(s)dsd\lambda d\theta,$$

$$V_5(t) = \int_0^t \int_{\theta-\tau_1(\theta)}^\theta \begin{bmatrix} e(\theta-\tau_1(\theta)) \\ \dot{e}(s) \end{bmatrix}^T \begin{bmatrix} T_{11} & T_{12} \\ \star & T_{22} \end{bmatrix} \begin{bmatrix} e(\theta-\tau_1(\theta)) \\ \dot{e}(s) \end{bmatrix} dsd\theta$$

$$+ \int_0^t \int_{\theta-\tau_2(\theta)}^\theta \begin{bmatrix} e(\theta-\tau_2(\theta)) \\ \dot{e}(s) \end{bmatrix}^T \begin{bmatrix} V_{11} & V_{12} \\ \star & V_{22} \end{bmatrix} \begin{bmatrix} e(\theta-\tau_2(\theta)) \\ \dot{e}(s) \end{bmatrix} dsd\theta,$$

$$V_6(t) = \int_{-\tau_1}^0 \int_{t+\theta}^t \dot{e}^T(s)T_{22}\dot{e}(s)dsd\theta + \int_{-\tau_2}^0 \int_{t+\theta}^t \dot{e}^T(s)V_{22}\dot{e}(s)dsd\theta.$$

By calculating the time derivation of $V_i(t)$ along the trajectory of system (25), we obtain

$$\begin{aligned}
\dot{V}_1(t) &\leq 2e^T(t)P\Big[-De(t) - He(t-\tau_2(t)) + Ag(e(t)) + Bg(e(t-\tau_1(t)))\Big] \\
&\quad + 2\Big|e(t)\Big|^T P\,(|\alpha|+|\beta|)\,\Big|g(e(t-\tau_1(t)))\Big| \\
&\leq -2e^T(t)PDe(t) - 2e^T(t)Q_0e(t-\tau_2(t)) + 2e^T(t)PAg(e(t)) + 2e^T(t)PB \\
&\quad \times g(e(t-\tau_1(t))) + e^T(t)Pe(t) + g^T(e(t-\tau_1(t)))\,(|\alpha|+|\beta|)^T\,P \\
&\quad \times (|\alpha|+|\beta|)\,g(e(t-\tau_1(t))) + 2\dot{e}^T(t)P\Big[-\dot{e}(t)+\dot{e}(t)\Big] \\
&\leq -2e^T(t)PDe(t) - 2e^T(t)Q_0e(t-\tau_2(t)) + 2e^T(t)PAg(e(t)) \\
&\quad + 2e^T(t)PBg(e(t-\tau_1(t))) + e^T(t)Pe(t) + ng^T(e(t-\tau_1(t)))\,(|\alpha|_s+|\beta|_s)^T \\
&\quad \times P\,(|\alpha|_s+|\beta|_s)\,g(e(t-\tau_1(t))) - 2\dot{e}^T(t)P\dot{e}(t) - 2\dot{e}^T(t)PDe(t) \\
&\quad -2\dot{e}^T(t)Q_0e(t-\tau_2(t)) + 2\dot{e}^T(t)PAg(e(t)) + 2\dot{e}^T(t)PBg(e(t-\tau_1(t))) \\
&\quad + \mu^{-1}n\dot{e}^T(t)P(|\alpha|_s+|\beta|_s)(|\alpha|_s+|\beta|_s)^T P\dot{e}(t) \\
&\quad + \mu\Big(g(e(t-\tau_1(t)))\Big)^T \Big(g(e(t-\tau_1(t)))\Big).
\end{aligned} \tag{28}$$

The proof of this remaining Corollary 3.4 is immediately follows from Theorem 3.1.   □

Remark 3.5. LMI approach is used in Theorem 3.1 and Corollary 3.4. When the size of LMI is increased, the feasible solution of the LMI can be easily obtained by using the effective interior point algorithms in convex optimization technique and the LMI toolbox in MATLAB, however the computational time get increased.

4. Illustrative Examples

Example 4.1. Consider the drive chaotic FCNNs system

$$\begin{cases} \dot{x}_i(t) = -d_ix_i(t) + \sum_{j=1}^n a_{ij}f_j(x_j(t)) + \sum_{j=1}^n b_{ij}f_j(x_j(t-\tau_1(t))) + I_i + \bigwedge_{j=1}^n \alpha_{ij} \\ \quad \times \int_{-\infty}^t k_j(t-s)f_j(x_j(s))ds + \bigvee_{j=1}^n \beta_{ij} \int_{-\infty}^t k_j(t-s)f_j(x_j(s))ds, \quad i \in \Lambda, \\ x_i(s) = \phi_i(s), \quad s \in (-\infty, 0], \end{cases} \tag{29}$$

with parameters defined as

$$
\begin{aligned}
\phi(s) &= (1, -1, -0.5)^T, \ s \in (-\infty, 0], \ f_j(x_j) = \frac{1}{2}\left(|x_j + 1| - |x_j - 1|\right), \ j = 1, 2, 3, \\
I_i &= 0.02, \ i = 1, 2, 3, \quad \tau_1(t) = 0.07 \, |\sin(t)|, \\
A &= \begin{bmatrix} 4.3 & -7.5 & -1.5 \\ -3 & 1.2 & -4.7 \\ -3.2 & 4.6 & -2.1 \end{bmatrix}, \quad B = \begin{bmatrix} 2.23 & -3.2 & -3.21 \\ -3.1 & 1.3 & -4.37 \\ -3.2 & 4.3 & 0.9 \end{bmatrix}, \\
D &= \begin{bmatrix} 3 & 0 & 0 \\ 0 & 2 & 0 \\ 0 & 0 & 2 \end{bmatrix}, \quad \alpha = \begin{bmatrix} 0.9 & -0.9 & 0.9 \\ 0.9 & 0.9 & -0.9 \\ -0.9 & 0.9 & 0.9 \end{bmatrix}, \\
\beta &= \begin{bmatrix} 0.9 & 0.9 & -0.9 \\ 0.9 & -0.9 & 0.9 \\ -0.9 & 0.9 & 0.9 \end{bmatrix}.
\end{aligned}
$$

The corresponding response system is designed as

$$
\begin{cases}
\dot{y}_i(t) = -d_i y_i(t) + \sum_{j=1}^n a_{ij} f_j(y_j(t)) + \sum_{j=1}^n b_{ij} f_j(y_j(t - \tau_1(t))) + I_i \\
\quad + \bigwedge_{j=1}^n \alpha_{ij} \int_{-\infty}^t k_j(t-s) f_j(y_j(s)) ds \\
\quad + \bigvee_{j=1}^n \beta_{ij} \int_{-\infty}^t k_j(t-s) f_j(y_j(s)) ds + u_i(t), \quad i \in \Lambda, \\
y_i(s) = \varphi_i(s), \quad s \in (-\infty, 0],
\end{cases}
\tag{30}
$$

where u is given by (10) and the initial condition is

$$
\varphi(s) = (0.5, -0.7, -1)^T, \quad s \in (-\infty, 0].
$$

Moreover, the sampling period is taken as $\tau_2 = 0.03$. By using the Matlab LMI toolbox to solve the LMI (12) in Theorem 3.1, it can be found that the LMI is feasible. Consequently, the controller gain matrix H is designed as follows:

$$
H = P^{-1} Q_0 = \begin{bmatrix} 0.1996 & -0.0567 & 0.1983 \\ -0.0502 & 0.1075 & -0.1013 \\ 0.2500 & -0.1443 & 0.3667 \end{bmatrix}.
\tag{31}
$$

By Theorem 3.1, systems (29) and (30) are asymptotically synchronized. The simulation results are illustrated in the Figures 4-7, in which the controller designed in (31) is applied.

Remark 4.2. The simulation results can be described as follows. Figures 2-3 describe the chaotic behavior in phase space of the drive system (29) and the response system (30) with control input (31), respectively. Figures 4-7 show that the state trajectories and error trajectories of the drive system (29) and the response system (30) with control input (31) to be asymptotically synchronized. Figures 8-11 provide the state trajectories and the error trajectories between the drive system (29) and the response system (30) without control input. One may observe that the drive system (29) and the response system (30) without control input cannot be synchronized. Figure 12 exhibits the response curve of control input $u(t)$. The numerical simulations clearly verify the effectiveness of the developed sampled-data control approach to the synchronization of chaotic FCNNs with discrete and unbounded distributed delays.
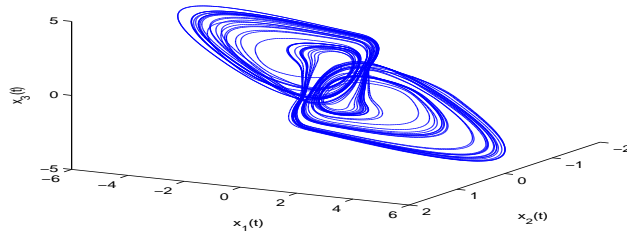
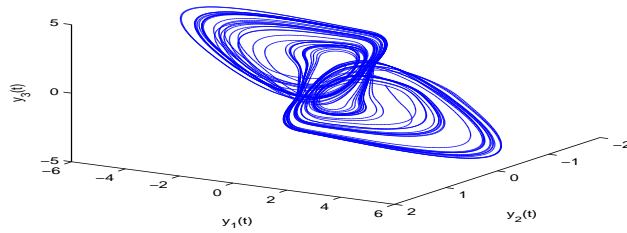FIGURE 2. Chaotic Attractor of Drive System (29)

FIGURE 3. Chaotic Attractor of Response System (30)
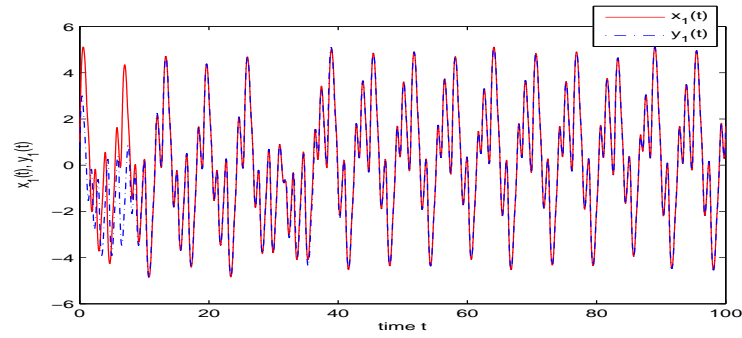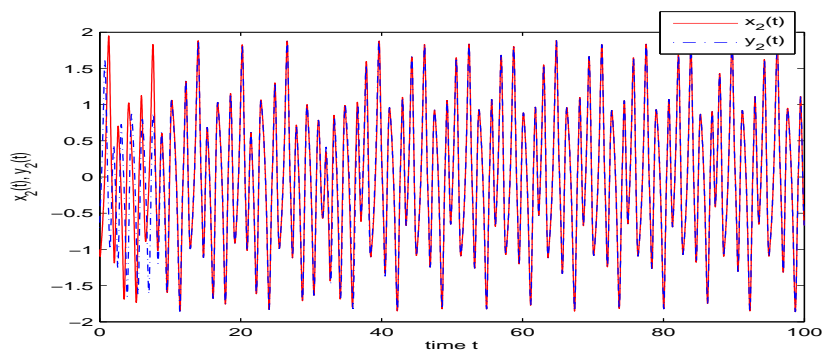with Control Input (31)

FIGURE 4. State Trajectories of Drive System (29) with State $x_1(t)$ and
Response System (30) with State $y_1(t)$ Through Control Input (31),
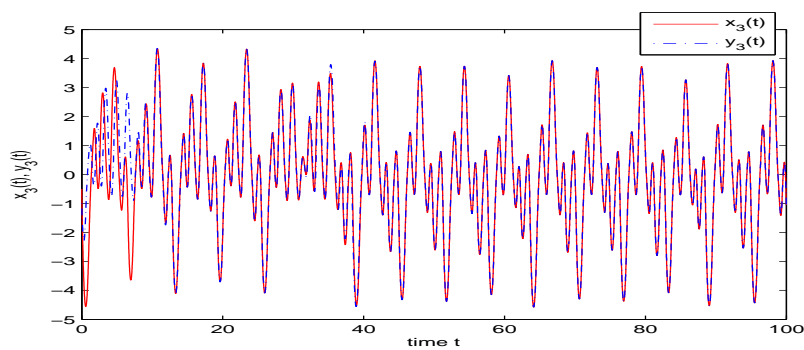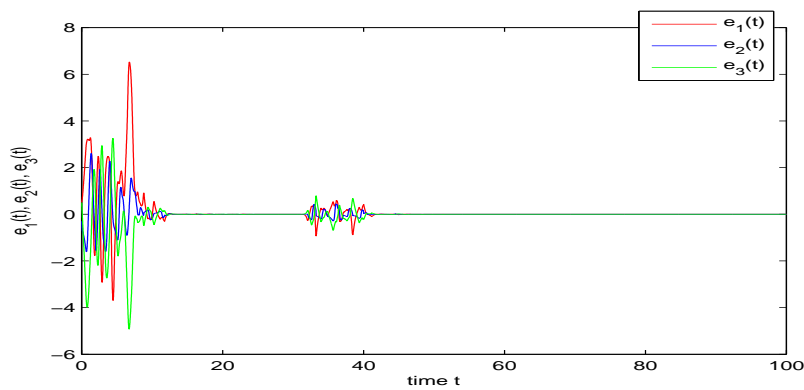when $\tau_2 = 0.03$

Example 4.3. [3] Consider the drive chaotic FCNNs system

$$
\begin{cases}
\dot{x}_i(t) = -d_i x_i(t) + \sum_{j=1}^n a_{ij} f_j(x_j(t)) + \sum_{j=1}^n b_{ij} f_j(x_j(t - \tau_1(t))) + I_i + \bigwedge_{j=1}^n \alpha_{ij} \\
\qquad \times \int_{-\infty}^t k_j(t-s) f_j(x_j(s)) ds + \bigvee_{j=1}^n \beta_{ij} \int_{-\infty}^t k_j(t-s) f_j(x_j(s)) ds, \quad i \in \Lambda, \\
x_i(s) = \phi_i(s), \quad s \in (-\infty, 0],
\end{cases}
\tag{32}
$$

FIGURE 5. State Trajectories of Drive System (29) with State $x_2(t)$ and Response System (30) with State $y_2(t)$ Through Control Input (31), when $\tau_2 = 0.03$

FIGURE 6. State Trajectories of Drive System (29) with State $x_3(t)$ and Response System (30) with State $y_3(t)$ Through Control Input (31), when $\tau_2 = 0.03$

FIGURE 7. Convergence Dynamics of Errors Between Drive System (29) and Response System (30) with Control Input (31), when $\tau_2 = 0.03$
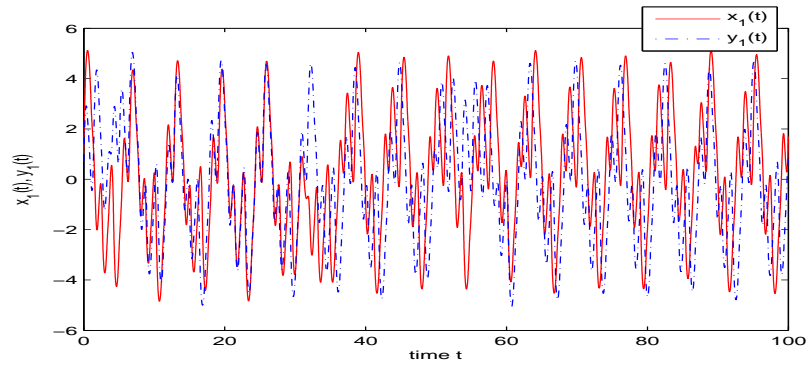
FIGURE 8. State Trajectories of Drive System (29) with State $x_1(t)$ and Response System (30) with State $y_1(t)$ without Control Input, when $\tau_2 = 0.03$
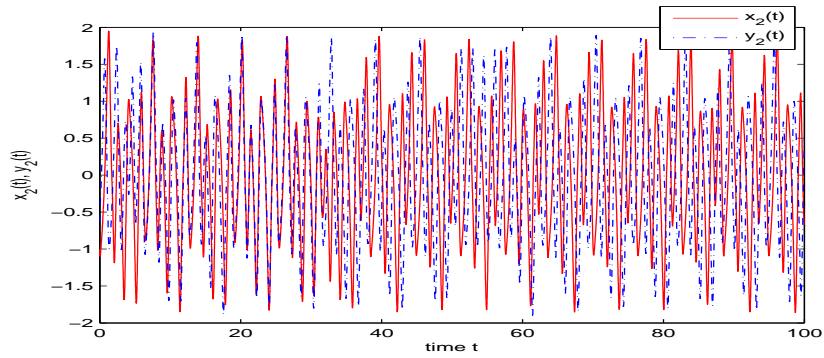

FIGURE 9. State Trajectories of Drive System (29) with State $x_2(t)$ and Response System (30) with State $y_2(t)$ without Control Input, when $\tau_2 = 0.03$
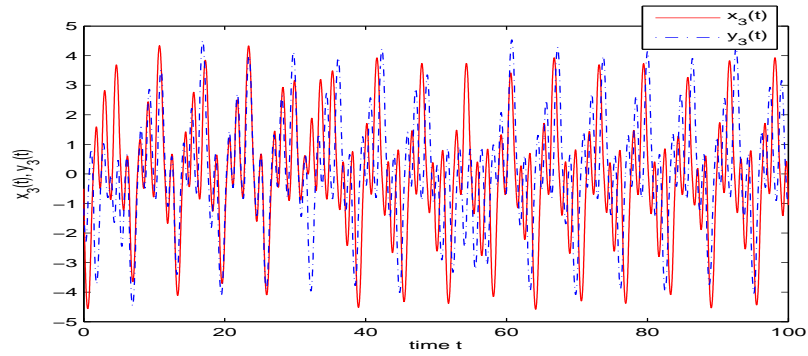

FIGURE 10. State Trajectories of Drive System (29) with State $x_3(t)$ and Response System (30) with State $y_3(t)$ without Control Input, when $\tau_2 = 0.03$
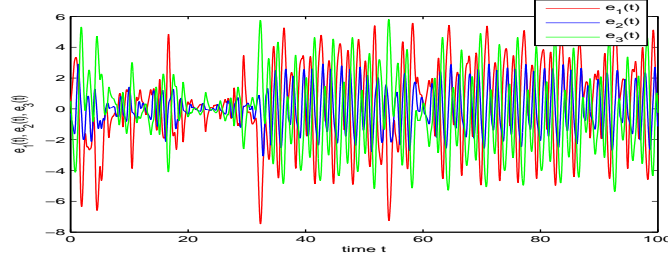
FIGURE 11. Convergence Dynamics of Errors Between Drive System (29) and Response System (30) without Control Input, when $\tau_2 = 0.03$
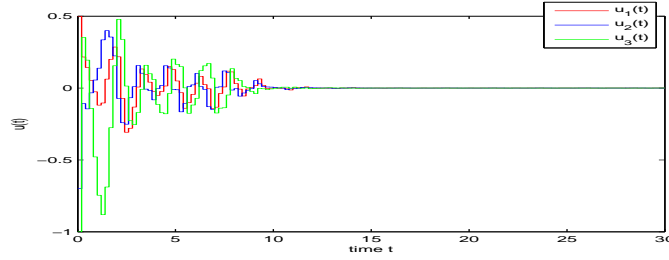

FIGURE 12. The Response Curve of Control Input $u(t)$, when $\tau_2 = 0.03$

with parameters defined as

$$\phi(s) = (1, -1, -0.5)^T, \ s \in (-\infty, 0], \ f_j(x_j) = \frac{1}{2}\big(|x_j + 1| - |x_j - 1|\big), \ j = 1, 2, 3,$$

$$I_i = 0, \ i = 1, 2, 3, \quad \tau_1(t) = 0.04 \, |\sin(t)|,$$

$$A = \begin{bmatrix} 1.25 & -3.21 & -3.2 \\ -3.2 & 1.1 & -4.4 \\ -3.2 & 4.4 & 1 \end{bmatrix}, \quad B = \begin{bmatrix} 4.3 & -7.5 & -3 \\ -3 & 1.2 & -5 \\ -3.2 & 4.5 & -2.3 \end{bmatrix},$$

$$D = \begin{bmatrix} 1 & 0 & 0 \\ 0 & 1 & 0 \\ 0 & 0 & 1 \end{bmatrix}, \quad \alpha = \beta = \begin{bmatrix} -1/32 & -1/32 & 1/32 \\ -1/32 & -1/32 & 1/32 \\ -1/32 & -1/32 & 1/32 \end{bmatrix}.$$

The corresponding response system is designed as

$$\begin{cases} \dot{y}_i(t) = -d_i y_i(t) + \sum_{j=1}^{n} a_{ij} f_j(y_j(t)) + \sum_{j=1}^{n} b_{ij} f_j(y_j(t - \tau_1(t))) + I_i \\ \qquad + \bigwedge_{j=1}^{n} \alpha_{ij} \int_{-\infty}^{t} k_j(t - s) f_j(y_j(s)) ds \\ \qquad + \bigvee_{j=1}^{n} \beta_{ij} \int_{-\infty}^{t} k_j(t - s) f_j(y_j(s)) ds + u_i(t), \quad i \in \Lambda, \\ y_i(s) = \varphi_i(s), \quad s \in (-\infty, 0], \end{cases} \tag{33}$$

where u is given by (10) and the initial condition is

$$\varphi(s) = (0.5, -0.7, -1)^T, \quad s \in (-\infty, 0].$$

Moreover, the sampling period is taken as $\tau_2 = 0.03$. By using the Matlab LMI toolbox to solve the LMI (12) in Theorem 3.1, it can be found that the LMI is

feasible. Consequently, the controller gain matrix H is designed as follows:

$$H = P^{-1}Q_0 = \begin{bmatrix} 0.4592 & -0.0205 & 0.1853 \\ -0.0145 & 0.4107 & -0.1235 \\ 0.1805 & -0.1701 & 0.6363 \end{bmatrix}.$$

(34)

By Theorem 3.1, systems (32) and (33) are asymptotically synchronized. The simulation results are illustrated in the Figure 13, in which the controller designed in (34) is applied.

	Maximum allowable upper bound (MAUB)
Theorem 1 [3]	$\tau = 0.0534$
Theorem 3.1	$\tau_1 = 0.0772$

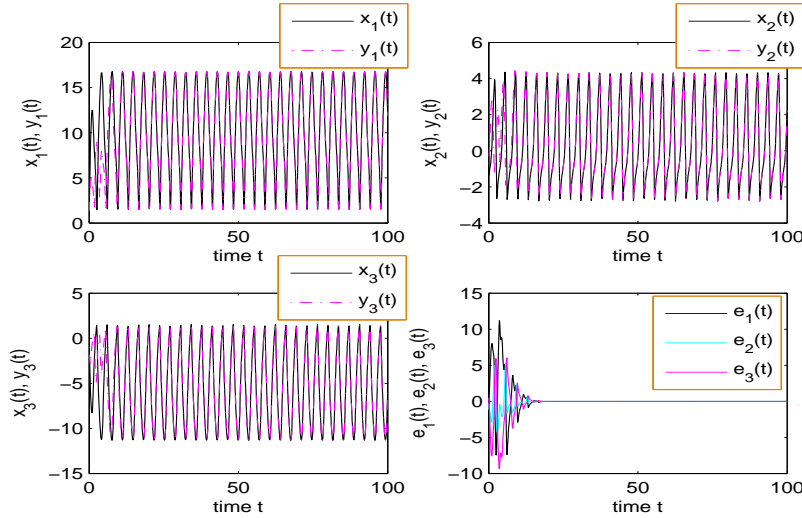TABLE 1. The MAUB τ_1 of Example 4.3

FIGURE 13. [3] State Trajectories and Error Trajectories of Drive System (32) and Response System (33) with Control Input (34), when $\tau_2 = 0.03$

Remark 4.4. The simulation results for comparison of [3] can be described as follows. Figure 13 shows that the state trajectories and error trajectories of the drive system (32) and the response system (33) with control input (34) to be asymptotically synchronized. Figure 14 provides the state trajectories and the error trajectories between the drive system (32) and the response system (33) without control input. One may observe that the drive system (32) and the response system (33) without control input cannot be synchronized.
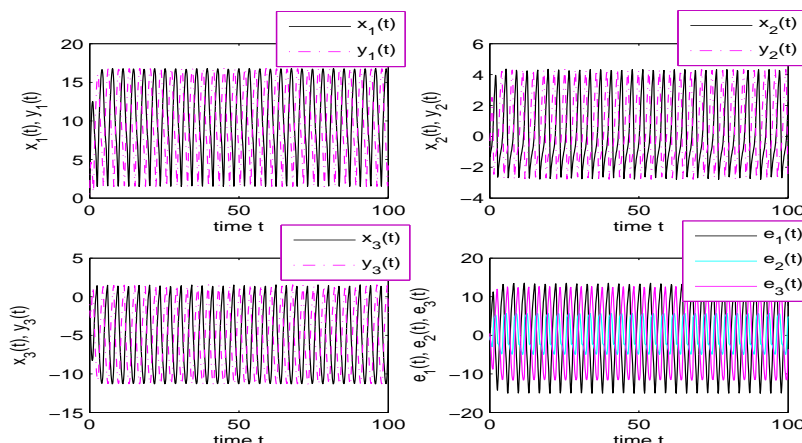
FIGURE 14. [3] State Trajectories and Error Trajectories of Drive
System (32) and Response System (33) without Control Input,
when $\tau_2 = 0.03$

5. Conclusions

In this paper, synchronization of chaotic FCNNs with discrete and unbounded distributed delays have been considered. Based on the sampled-data control techniques, Lyapunov stability theory and LMI approach, sufficient conditions have been developed to guarantee synchronization of coupled FCNNs. Moreover, the result is novel for synchronization of chaotic FCNNs with discrete and unbounded distributed delays based on the sampled-data control rather than existing literatures [3, 12, 13, 24, 34, 35]. Further, in the absence of unbounded distributed delay the results have been derived by employing a Lyapunov-Krasovskii functional and using the LMI approach based on the sampled-data control. The effectiveness of the proposed results and comparison have been demonstrated through two numerical examples and simulations well.

Moreover, impulsive effects may be unavoidable while implementing electronic networks in the cases of switching phenomenon, frequency change or other sudden noise etc. In future, the above results may be extended further with impulsive effects by using delay partitioning and convex combination technique to obtain less conservative results.

REFERENCES

[1] A. Arunkumar, R. Sakthivel, K. Mathiyalagan and S. Marshal Anthoni, *Robust state estimation for discrete-time BAM neural networks with time-varying delay*, Neurocomputing, **131** (2014), 171-178.

[2] A. Arunkumar, R. Sakthivel, K. Mathiyalagan and Ju H. Park, *Robust stochastic stability of discrete-time fuzzy Markovian jump neural networks*, ISA Transactions, **53** (2014), 1006–1014.

[3] P. Balasubramaniam, M. Kalpana and R. Rakkiyappan, *Linear matrix inequality approach for synchronization control of fuzzy cellular neural networks with mixed time delays*, Chinese Physics B, **21** (2012): 048402.

[4] S. Boyd, L. E. Ghaoui, E. Feron and V. Balakrishnan, *Linear Matrix Inequalities in Systems and Control Theory* (SIAM, Philadelphia, 1994).

[5] T. L. Carroll and L. M. Pecora, *Synchronization chaotic circuits*, IEEE Trans. Circuits Syst., **38** (1991), 453–456.

[6] L. O. Chua and L. Yang, *Cellular neural networks: theory*, IEEE Trans. Circuits Syst., **35** (1988), 1257-1272.

[7] L. O. Chua and L. Yang, *Cellular neural networks: applications*, IEEE Trans. Circuits Syst., **35** (1988), 1273-1290.

[8] X. Feng, F. Zhang and W. Wang, *Global exponential synchronization of delayed fuzzy cellular neural networks with impulsive effects*, Chaos Solitons Fractals., **44** (2011), 9–16.

[9] T. Feuring, J. J. Buckley, W. M. Lippe and A. Tenhagen, *Stability analysis of neural net controllers using fuzzy neural networks*, Fuzzy Sets and Systems, **101** (1999), 303–313.

[10] E. Fridman, A. Seuret and J. P. Richard, *Robust sampled-data stabilization of linear systems: an input delay approach*, Automatica, **40** (2004), 1441–1446.

[11] Q. Gan and Y. Liang, *Synchronization of chaotic neural networks with time delay in the leakage term and parametric uncertainties based on sampled-data control*, J. Franklin Inst., **349** (2012), 1955–1971.

[12] Q. Gan, R. Xu and P. Yang, *Synchronization of non-identical chaotic delayed fuzzy cellular neural networks based on sliding mode control*, Commun. Nonlinear Sci. Numer. Simul., **17** (2012), 433–443.

[13] Q. Gan, R. Xu and P. Yang, *Exponential synchronization of stochastic fuzzy cellular neural networks with time delay in the leakage term and reaction-diffusion*, Commun. Nonlinear Sci. Numer. Simul., **17** (2012), 1862–1870.

[14] K. Gu, An integral inequality in the stability problem of time-delay systems, in *Proceedings of the 39th IEEE Conference on Decision and Control Sydney*, Australia (2000), 2805–2810.

[15] S. Lee, V. Kapila, M. Porfiri and A. Panda, *Master-slave synchronization of continuously and intermittently coupled sampled-data chaotic oscillators*, Commun. Nonlinear Sci. Numer. Simul., **15** (2010), 4100–4113.

[16] T. Li, S. Fei and Q. Zhu, *Design of exponential state estimator for neural networks with distributed delays*, Nonlinear Anal. Real World Appl., **10** (2009), 1229–1242.

[17] N. Li, Y. Zhang, J. Hu and Z. Nie, *Synchronization for general complex dynamical networks with sampled-data*, Neurocomputing, **74** (2011), 805–811.

[18] Z. Liu, H. Zhang and Z. Wang, *Novel stability criterions of a new fuzzy cellular neural networks with time-varying delays*, Neurocomputing, **72** (2009), 1056–1064.

[19] J. Lu and D. J. Hill, *Global asymptotical synchronization of chaotic Lur'e systems using sampled data: a linear matrix inequality approach*, IEEE Trans. Circuits Syst. II, **55** (2008), 586–590.

[20] K. Mathiyalagan, S. Hongye and R. Sakthivel, *Robust stochastic stability of discrete-time Markovian jump neural networks with leakage delay*, Zeitschrift Fur Naturforschung Section A-A Journal of Physical Sciences, **69** (2014), 70–80.

[21] K. Mathiyalagan, R. Sakthivel and S. Hongye, *Exponential state estimation for discrete-time switched genetic regulatory networks with random delays*, Canad. J. Phys., **92** (2014), 976–986.

[22] L. M. Pecora and T. L. Carroll, *Synchronization in chaotic systems*, Phys. Rev. Lett., **64** (1990), 821–824.

[23] L. M. Pecora, T. L. Carroll, G. A. Johnson, D. J. Mar and J. F. Heagy, *Fundamentals of synchronization in chaotic systems, concepts, and applications*, Chaos, **7** (1997), 520–543.

[24] Y. Ping and L. Teng, *Exponential synchronization of fuzzy cellular neural networks with mixed delays and general boundary conditions*, Commun. Nonlinear Sci. Numer. Simul., **17** (2012), 1003–1011.

[25] R. Sakthivel, R. Raja and S. Marshal Anthoni, *Linear matrix inequality approach to stochastic stability of uncertain delayed BAM neural networks*, IMA J Appl Math., **78** (2013), 1156–1178.

[26] E. N. Sanchez and J. P. Perez, *Input-to-state stability (ISS) analysis for dynamic neural networks*, IEEE Trans. Circuits Syst. I, **46** (1999), 1395-1398.

[27] F. O. Souza, R. M. Palhares and P. Y. Ekel, *Asymptotic stability analysis in uncertain multi-delayed state neural networks via Lyapunov-Krasovskii theory*, Math. Comput. Modelling, **45** (2007), 1350–1362.

[28] F. O. Souza, R. M. Palhares and P. Y. Ekel, *Novel stability criteria for uncertain delayed Cohen-Grossberg neural networks using discretized Lyapunov functional*, Chaos Solitons Fractals, **41** (2009), 2387–2393.

[29] F. O. Souza, R. M. Palhares and P. Y. Ekel, *Improved asymptotic stability analysis for uncertain delayed state neural networks*, Chaos Solitons Fractals, **39** (2009), 240–247.

[30] Y. Tang and J. Fang, *Robust synchronization in an array of fuzzy delayed cellular neural networks with stochastically hybrid coupling*, Neurocomputing, **72** (2009), 3253–3262.

[31] T. Yang and L. B. Yang, *Global stability of fuzzy cellular neural network*, IEEE Trans. Circuits Syst. I, **43** (1996), 880–883.

[32] T. Yang, L. B. Yang, C. W. Wu and L. O. Chua, Fuzzy cellular neural networks: Theory, in *Proceedings of the IEEE International Workshop on Cellular Neural Networks and Applications*, (1996), 181–186.

[33] T. Yang, L. B. Yang, C. W. Wu and L. O. Chua, Fuzzy cellular neural networks: Applications, in *Proceedings of the IEEE International Workshop on Cellular Neural Networks and Applications*, (1996), 225–230.

[34] J. Yu, C. Hu, H. Jiang and Z. Teng, *Exponential lag synchronization for delayed fuzzy cellular neural networks via periodically intermittent control*, Math. Comput. Simulation, **82** (2012), 895–908.

[35] F. Yu and H. Jiang, *Global exponential synchronization of fuzzy cellular neural networks with delays and reaction-diffusion terms*, Neurocomputing, **74** (2011), 509–515.

[36] L. A. Zadeh, *Fuzzy Sets*, Information and Control, **8** (1965), 338–353.

[37] C. Zhang, Y. He and M. Wu, *Exponential synchronization of neural networks with time-varying mixed delays and sampled-data*, Neurocomputing, **74** (2010), 265–273.

P. Balasubramaniam-pour*, Department of Mathematics, Gandhigram Rural Institute - Deemed University, Gandhigram - 624 302, Tamilnadu, India
    E-mail address: balugru@gmail.com

K. Ratnavelu, Institute of Mathematical Sciences, Faculty of Science, University of Malaya - 50603, Kuala Lumpur, Malaysia
    E-mail address: kururatna2012@gmail.com

M. Kalpana, Institute of Mathematical Sciences, Faculty of Science, University of Malaya - 50603, Kuala Lumpur, Malaysia
    E-mail address: kalpana.nitt@gmail.com

*Corresponding author